

Intepretation of Faradaic Impedance for Corrosion Monitoring

M. Itagaki, A. Taya, M. Imamura, R. Saruwatari, and K. Watanabe

Science University of Tokyo, Faculty of Science and Technology
Noda-shi, Chiba, 278-8510, JAPAN

A polarization resistance is generally used to estimate the corrosion rate in the corrosion monitoring by an electrochemical impedance method. When the Faradaic impedance has a time constant due to the reaction intermediate, the electrochemical impedance describes more than one loop on the complex plane. For example, the electrochemical impedance of iron in acidic solution shows capacitive and inductive loops on the complex plane. In this case, the charge transfer resistance and the polarization resistance are determined at middle and low frequency ranges, respectively. Which should be selected for corrosion resistance in corrosion monitoring, the charge transfer resistance or the polarization resistance? In the present paper, the above-mentioned question is examined theoretically and experimentally.

Keywords : electrochemical impedance, Faradaic impedance, inductive loop, corrosion monitoring.

1. Introduction

An electrochemical impedance method has been used to the corrosion investigations. The simplest electrochemical impedance has one time constant due to polarization resistance R_p and the capacitance of the electric double layer C_{dl} , and is presented by the equivalent circuit in Fig. 1(a). In this case the electrochemical impedance Z shows a capacitive loop on the complex plane (Fig. 1(c)). The intersections of the loop and the real axis give (1) the solution resistance R_{sol} at high frequency limit and (2) the $R_{sol} + R_p$ at low frequency limit. In the corrosion monitoring, the electrochemical impedances are measured at sufficient high and low frequencies, and the R_p is obtained by the difference of the amplitudes of two impedances. This R_p corresponds to the corrosion resistance R_{cor} in the corrosion monitoring and the R_p is in inverse proportion to the corrosion rate. On the other hand, the electrochemical impedances of some metal describe the second loop in Fig. 1(d)-(f). The second loop at low frequency range in Fig. 1(d) is called inductive loop.^{1),2)} The impedance in Fig. 1(f) represents a negative resistance at low frequency range. The negative resistance is observed at passivation³⁾ and transpassive dissolution^{4),5)} of some metals. These impedance in Figs. 1(d)-(f) have three interactions, namely, (1) R_{sol} at high frequency limit, (2) $R_{sol} + R_p$ at low frequency limit, and (3) R_{sol} plus the charge transfer resistance R_{ct} at middle frequency range. The R_p is usually adopted to estimate the corrosion rate in the corrosion monitoring. However, it has not been clarified

in the estimation of the corrosion rate whether the R_{ct} or the R_p should be selected for the R_{cor} . Epelboin *et al.*⁶⁾ studied the inductive behavior of iron in sulfuric acid solution with propargylic alcohol, and reported that the $1/R_{ct}$ gave the corrosion rate obtained by the weight loss of the iron. Haruyama *et al.*⁷⁾ derived the mathematical expression of Faradaic impedance of corroding electrode under some conditions, i.e., diffusion control, inhibitor adsorption, etc. Furthermore, they⁶⁾ concluded that R_{ct} should be R_{ct} by the comparison of the derived theory with the other methods to estimate corrosion rate. Lorenz *et al.*⁸⁾ investigated the relations of R_{ct} and R_p with the dissolution rate of iron by atomic absorption spectrophotometry, and disagreed with the interpretation of R_{ct} by Epelboin *et al.*⁶⁾ Itagaki *et al.*^{9),10)} compared R_{ct} with the dissolution rate of iron electrode in sulfuric acid solution containing halide ions and reported the good correlation between $1/R_{ct}$ and dissolution rate.

The second loop at low frequency range in Figs. 1(d)-(f) can be presented by Faradaic impedance Z_F . In the present paper, the physical meanings of R_{ct} and R_p in the Faradaic impedance for metal dissolution are discussed. Furthermore, the R_{ct} for iron and nickel electrodes in sulfuric acid solution are compared with the dissolution rate in order to verify the theoretical expression.

2. Experimental

2.1 Electrochemical impedance

The measurements for iron electrode were described in

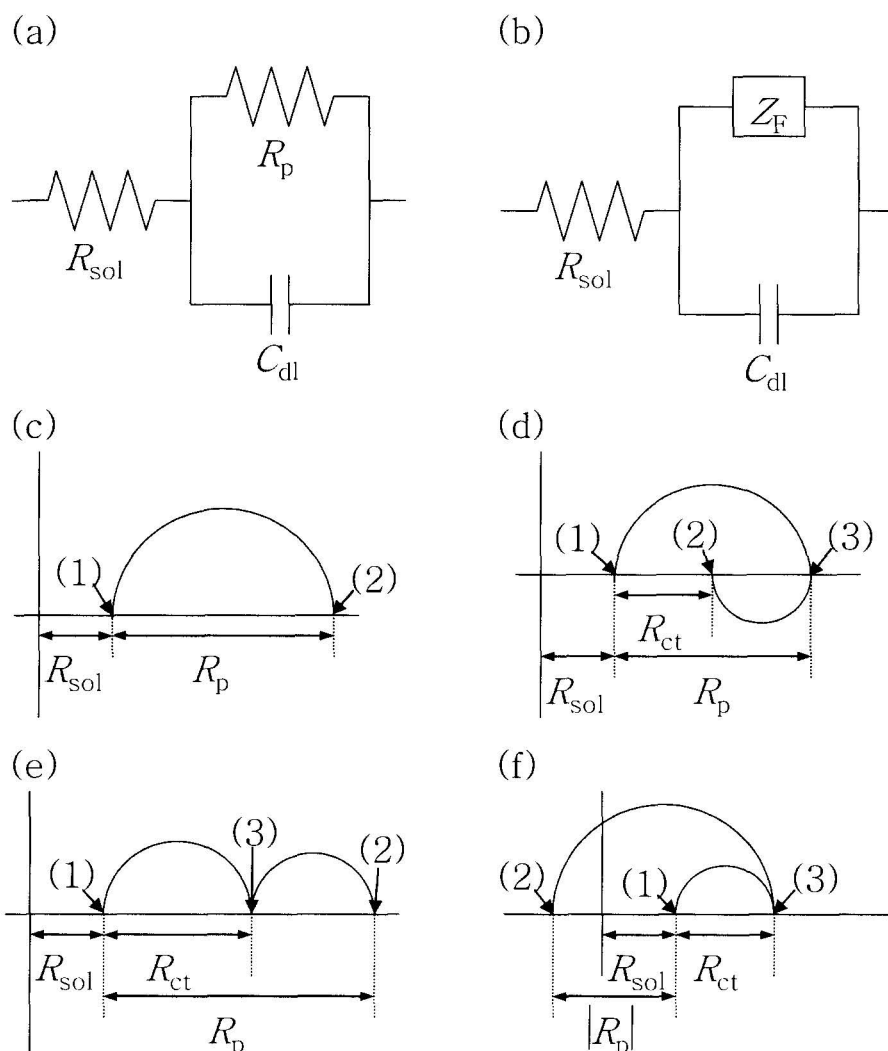


Fig. 1. Equivalent circuits and impedances.

- (a) The equivalent circuit of the simple electrochemical impedance.
- (b) The equivalent circuit of the impedance with inductive loop.
- (c) The scheme of impedance with capacitive loop by the equivalent circuit (a).
 - (1): the solution resistance R_{sol} at high frequency limit.
 - (2): the sum of R_{sol} and the polarization resistance R_p at low frequency limit.
- (d) The scheme of impedance with inductive loop by the equivalent circuit (b).
 - (1): R_{sol} at high frequency limit.
 - (2): $R_{sol} + R_p$ at low frequency limit.
 - (3): the sum of R_{sol} and the charge transfer resistance R_{ct} at middle frequency.
- (e) The scheme of impedance with second capacitive loop.
- (f) The scheme of impedance with negative resistance.

the previous paper.¹⁰⁾ Nickel disk electrode was used for the working electrode. The area of the nickel electrode was 0.71 cm^2 . The working electrode was polished by emery paper of #2000, and rinsed by methanol and distilled water successively before the measurement. The counter and reference electrodes were Pt and a saturated

KCl/AgCl/Ag (SSE), respectively. The electrolyte solution was a mixture of $0.5 \text{ mol/dm}^3 \text{ H}_2\text{SO}_4$ and $0.5 \text{ mol/dm}^3 \text{ Na}_2\text{SO}_4$ and its pH was adjusted at 1. The electrochemical impedance was determined by using a potentiostat (Hokuto, HA501G) and a frequency response analyzer (NF, FRA5020). The imposed ac signal was 10mV.

2.2 Determination of Ni(II) dissolution rate

How to determine the dissolution rate of Fe(II) is referred to the previous paper.¹⁰⁾ The concentration of Ni(II) dissolved from nickel electrode, which is polarized at an arbitrary potential, was determined by a spectrophotometer (Shimazu, UV2100S). The reagent was dimethylglyoxime. The wavelength to determine was 445 nm. The Ni(II) dissolution rate was calculated from the Ni(II) concentration, the solution volume, the polarized time, the area of the working electrode.

3. Results and discussion

3.1 Typical Faradaic impedances on the complex plane

In this section, relation between the Faradaic impedance and the adsorption is discussed. When the adsorbed intermediates exist on the electrode at the fractional coverage θ .

$$I = f(E, \theta) \tag{1}$$

Since the corrosion proceeds with both anodic and cathodic reactions, electrode reaction contains the adsorbed intermediates for both reactions. In the present paper, only one adsorption is considered for the simplicity. From eq. (1), a small modulation of current ΔI is:

$$\Delta I = a_1 \Delta E + a_2 \Delta \theta, \tag{2}$$

where $a_1 = (\partial I / \partial E)_\theta$ and $a_2 = (\partial I / \partial \theta)_E$. Therefore, the admittance A_F of the electrode is:

$$A_F = \Delta I / \Delta E = a_1 + a_2 \Delta \theta / \Delta E. \tag{3}$$

Assuming that the adsorption-desorption process is linear, $\Delta \theta / \Delta E$ in the frequency domain is written as follows:¹¹⁾

$$\Delta \theta / \Delta E = a_\theta / \{ 1 + j \omega \tau \} \tag{4}$$

where a_θ is a constant, j is an imaginary number, ω is

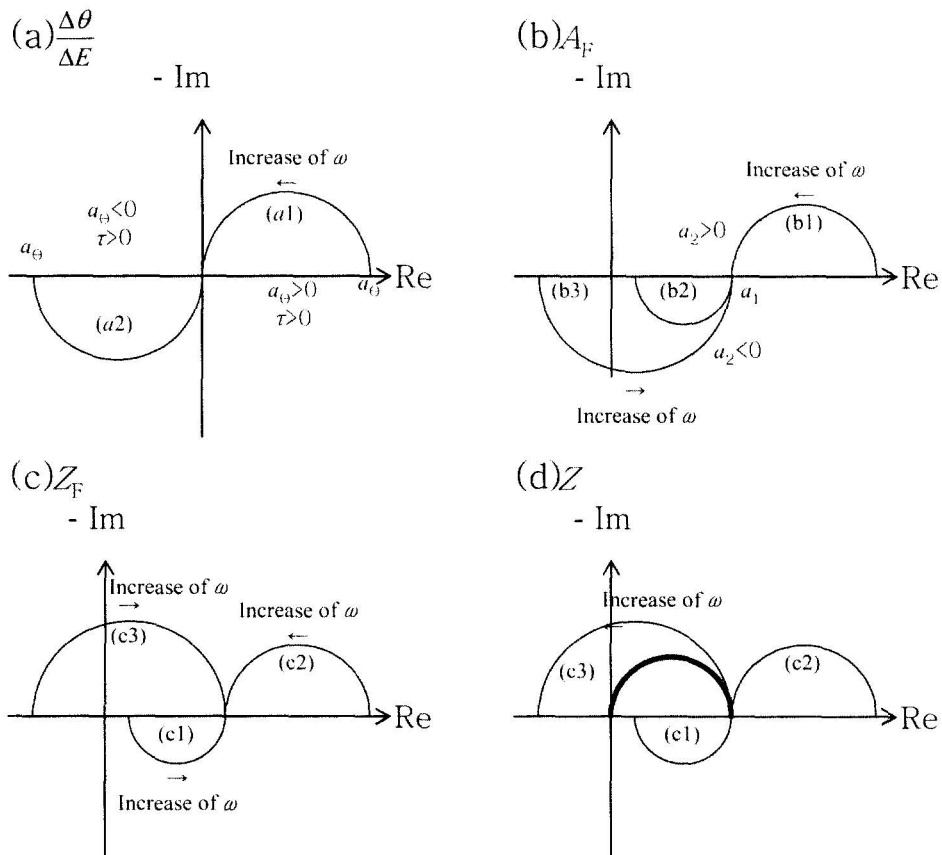


Fig. 2. Scheme of various parameters in the frequency domain: (a) $\Delta\theta/\Delta E$, (b) Admittance A_F , (c) Faraday impedance Z_F , (d) Impedance Z .

an angular frequency ($\omega = 2\pi f$, f is the frequency), τ is the time constant of adsorption-desorption. The schemes of $\Delta\theta / \Delta E$ on the complex plane are depicted in Fig. 2(a). The $\Delta\theta / \Delta E$ describes semicircle in the fourth quadrant (real and imaginary parts are positive and negative respectively.) when $a_\theta > 0$ and $\tau > 0$. The $\Delta\theta / \Delta E$ converges to the origin at high frequency limit since f is much larger than $1/\tau$ and since the adsorption-desorption process can not follow the potential modulation. Contrary to this, $\Delta\theta$ can symphonizes the ΔE at low frequency limit, and $\Delta\theta / \Delta E$ converges to a_θ on the real axis. On the other hand, the $\Delta\theta / \Delta E$ describes semicircle in the second quadrant (real and imaginary parts are negative and positive respectively.) when $a_\theta < 0$ and $\tau > 0$. The negative value of a_θ indicates that the coverage of reaction site decreases by imposing the noble potential.

The A_F is derived by the eq. (3) and $\Delta\theta / \Delta E$ when $a_\theta > 0$, and presented in Fig. 2(b). When $a_2 > 0$, A_F describes a semicircle at fourth quadrant (case (b1)). When $a_2 < 0$, A_F describes a semicircle at first quadrant (both real and imaginary parts are positive.) as the case (2). If $a_1 + a_\theta a_2 < 0$, A_F takes negative real value at low frequency range. The Faradaic impedance Z_F is reciprocal of the A_F and the loci in these cases are described in Fig. 2(c). The Z_F 's show the inductive loop (c1), the capacitive loop (c2) and negative resistance (c3), and corresponds to the A_F 's in these cases (b1), (b2) and (b3), respectively. The loci of all Z_F converge to $1/a_1$ at high frequency limit, and the $1/a_1$ is the charge transfer resistance R_{ct} . Therefore, the R_{ct} means the Faradaic impedance when the adsorption is not influenced by a.c. modulation. On the other hand, the Z_F at low frequency limit is the polarization resistance R_p . The R_p means the Z_F when the coverage of adsorbed species change by a.c. modulation. These considerations lead to the conclusion that $1/R_{ct}$ is related to the corrosion rate at d.c. condition and that $1/R_p$ corresponds to the slope dI/dE of I- E curve. The electrode impedance Z shows the capacitive loop due to C_{dl} at high frequency region in Fig. 2(d).

$$1/Z = 1/Z_F + j\omega C_{dl} \quad (5)$$

3.2 Relation of R_{ct} with dissolution rate

Typical three impedances of iron and nickel during dissolution are shown in Fig. 3. Fig. 3(a) shows the impedance of iron at -0.2V in sulfuric acid solution (pH 1) containing 0.03 mol/dm^3 NaI. The impedance in Fig. 3 (a) shows inductive loop at low frequency region. This inductive loop is related to the time constant of adsorption-desorption as mentioned in the previous section. Figs. 3(b)

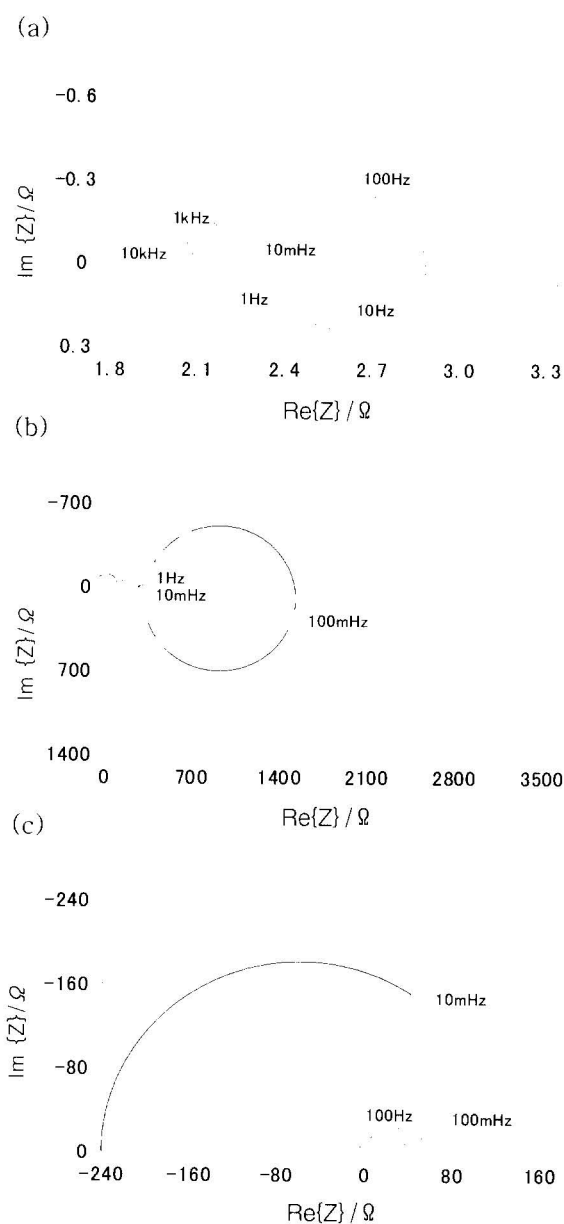


Fig. 3. (a) Electrochemical impedance of iron at -0.2 V vs. SSE in sulfuric acid solution (pH 1) containing 0.03 mol/dm^3 NaI. (b) Electrochemical impedance of nickel at 1.3 V in sulfuric acid solution (pH 1). (c) Electrochemical impedance of nickel at 1.5 V in sulfuric acid solution (pH 1).

and (c) show the impedances of nickel at 1.3 V and 1.5 V, respectively, in the sulfuric acid solution of pH 1. The impedance in Fig. 3(b) shows a second capacitive loop and an inductive loop. The impedance in Fig. 3(c) shows a negative resistance.

Fig. 4 shows the log-log plots of $1/R_{ct}$ and the dissolution rate V_{diss} at various experimental conditions. Open and solid symbols denote the results for iron¹⁰⁾ and nickel

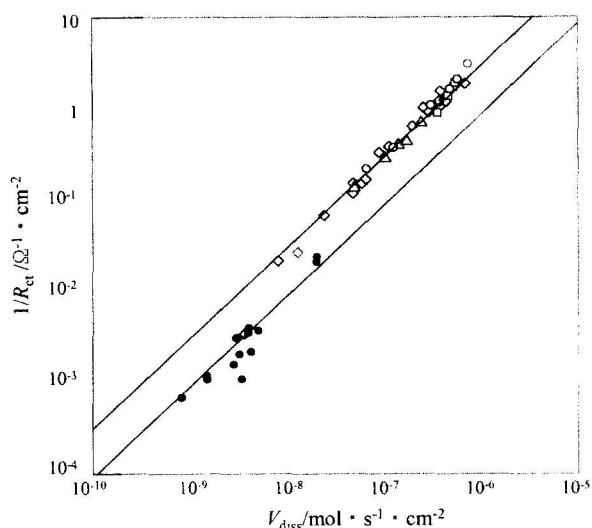


Fig. 4. Relation between R_{ct} and dissolution rate.
 ○: R_{ct} of iron when electrolyte was sulfuric acid solution (pH 1).
 □: R_{ct} of iron when electrolyte was sulfuric acid solution (pH 1) containing 0.1 kmol/m^3 NaCl.
 ◇: R_{ct} of iron when electrolyte was sulfuric acid solution (pH 1) containing $0.01\text{-}0.3 \text{ kmol/m}^3$ NaI.
 △: R_{ct} of iron when electrolyte was sulfuric acid solution (pH 1) containing 0.05 kmol/m^3 propargylic alcohol.
 ●: R_{ct} of nickel when electrolyte was sulfuric acid solution (pH 1).

respectively. The slopes for both iron and nickel are unity in Fig. 4, indicating the linear relationship between $1/R_{ct}$ and V_{diss} . On the basis of the above-mentioned results, the R_{ct} should be used to estimate the corrosion rate strictly in the electrochemical impedance method. Especially the corrosion rate may be overestimated by using R_p when the large inductive loop is observed. It should be necessary to select the suitable frequency to measure the corrosion resistance depending on the corrosion mechanism.

4. Summary

Relation of R_{ct} with the dissolution rate was investigated for iron and nickel electrodes that show second loop on the complex plane. Comparison of R_{ct} with the dissolution rate determined by the spectrophotometer leads to the conclusion: R_{ct} has simple relation with the dissolution rate of metal. Furthermore investigation is necessary for the following electrodes which have more than one time constant: the electrode covered with oxide film, the electrode with localized corrosion, and diffusion-controlled electrode.

References

1. I. Epelboin and M. Keddam, *J. Electrochem. Soc.*, **117**, 1052 (1970).
2. M. Itagaki, M. Tagaki, and K. Watanabe, *Electrochem. Acta*, **41**, 1201 (1996).
3. N. Benzekri, M. Keddam, and H. Takenouti, *Electrochem. Acta.*, **34**, 1159 (1989).
4. M. Keddam, H. Takenouti, and N. Yu, *J. Electrochem. Soc.*, **132**, 2561 (1985).
5. M. Itagaki, N. Hasebe, and K. Watanabe, *Passivity and Localized Corrosion, Electrochemical Society Proceeding Volume 99-27*, 103 (1999).
6. I. Epelboin, M. Keddam, and H. Takenouti, *J. Appl. Electrochem.*, **2**, 71 (1972).
7. S. Haruyama, T. Tsuru, and M. Anan, *Boshoku Gijutsu.*, **27**, 449 (1978).
8. W. J. Lorenz and F. Mansfeld, *Corros. Sci.*, **21**, 647 (1981).
9. M. Itagaki, M. Imamura, A. Taya, and K. Watanabe, *Zairyo to kankyo*, in press.
10. M. Itagaki, M. Imamura, A. Taya, and K. Watanabe, *Electrochim. Acta*, submitted.
11. M. Itagaki and K. Watanabe, *Denki Kagaku (presently Electrochemistry)*, **65**, 758 (1997).